Published in final edited form as:
*Bioconjug Chem*. 2010 April 21; 21(4): 764–773. doi:10.1021/bc900553n.

# Design, Synthesis and Biological Evaluation of a Robust, Biodegradable Dendrimer

**Derek G. van der Poll**[†], **Heidi M. Kieler-Ferguson**[†], **William C. Floyd**[†], **Steven J. Guillaudeu**[†], **Katherine Jerger**[‡], **Francis C. Szoka**[‡,*], and **Jean M. Fréchet**[†,*]

[†]College of Chemistry, University of California, Berkeley, California 94720-1460

[‡]Department of Biopharmaceutical Sciences and Pharmaceutical Chemistry, University of California, San Francisco, California 94143-0446

## Abstract

PEGylated dendrimers are attractive for biological applications due to their tunable pharmacokinetics and ability to carry multiple copies of bioactive molecules. The rapid and efficient synthesis of a robust and biodegradable PEGylated dendrimer based on a polyester-polyamide hybrid core is described. The architecture is designed to avoid destructive side-reactions during dendrimer preparation while maintaining biodegradability. Therefore, a dendrimer functionalized with doxorubicin (Dox) was prepared from commercial starting materials in nine, high-yielding linear steps. Both the dendrimer and Doxil™ were evaluated in parallel using equimolar dosage in the treatment of C26 murine colon carcinoma, leading to statistically equivalent results with most mice tumor-free at the end of the sixty day experiment. The attractive features of this dendritic drug carrier are its simple synthesis, biodegradability, and versatility for application to a variety of drug payloads with high drug loadings.

## INTRODUCTION

The use of macromolecular carriers for the delivery of chemotherapeutics originated from the hypothesis that polymers may be used to improve both the solubility and the blood circulation time of small molecule drugs (1,2). It was later discovered that macromolecules have the additional benefit of increased accumulation in tumor tissue as a result of the leaky vasculature surrounding rapidly growing neoplasm—a concept known as the enhanced permeation and retention (EPR) effect (3,4). Thus, macromolecular carriers can provide both enhanced pharmacokinetics and a passive targeting mechanism, characteristics that may be used to increase the efficacy of small molecule drugs. To this end, carrier systems such as linear polymers, micellar assemblies, liposomes, polymersomes and dendrimers have been studied in an effort to identify an ideal drug carrier (5–14). Important design features (9) include a long blood circulation time, high tumor-accumulation, high drug-loading, low toxicity, low polydispersity index and simple preparation. Considering the above criteria, PEGylated dendrimers (15,16) constitute an attractive platform because their size and degree of branching can be precisely controlled and they possess multiple functional appendages for the attachment of both drugs and solubilizing groups. Dendritic drug carriers based on polyesters (17–19), polyamines (20,21), melamines or triazines (22–24), PAMAM (25–30), and other polyamides (31–33) have all been explored and recently reviewed (14). Polyesters constitute a very

[*]Corresponding Authors szoka@cgl.ucsf.edu and frechet@berkeley.edu.

**Supporting Information Available:** Additional synthetic details and characterization. This material is available free of charge via the Internet at http://pubs.acs.org.

attractive class of materials because they are biodegradable; however, the hydrolytic susceptibility of the ester bond can make the synthesis of drug conjugates somewhat challenging. The hydrolysis rates of polyesters can vary dramatically depending on the hydrophobicity of the monomer, steric environment, and the reactivity of functional groups located within the dendrimer (34). In contrast, polyamide and polyamine dendrimers can withstand a much wider selection of synthetic manipulations, but they do not degrade as easily in the body and thus they may be more prone to long-term accumulation *in vivo* (35). Currently, challenges facing the biological application of dendrimers are their lengthy syntheses and the need to develop nontoxic, biodegradable dendrimers that are still resilient to the reaction conditions encountered during their synthesis and modification. As a result, accessing a universal, biodegradable, highly soluble, unimolecular carrier capable of achieving a high drug loading and low polydispersity has remained a challenge.

In recent studies, we have determined that a family of polyester-core dendrimer based on a 2,2-bis(hydroxymethyl) propanoic acid (bis-HMPA) monomer unit, typically functionalized with eight 5 kDa poly(ethylene glycol) (PEG) chains (18) is biocompatible and that it is capable of high drug loading while facilitating high tumor accumulation through its long circulation half-life. An asymmetric bis-HMPA PEGylated dendrimer functionalized with doxorubicin via a pH sensitive acyl hydrazone bond demonstrated outstanding antitumor activity in mice bearing murine C26 colon carcinoma (17). Despite these promising *in vivo* results, further evaluation of this asymmetric carrier in biological models was slowed by its lengthy synthesis (37). Therefore we sought to transpose the beneficial features (9) of this PEGylated dendrimer onto a simpler and more readily prepared carrier. Initial approaches involved simplified multifunctional dendrimers based on bis-HMPA (38,39); however, some issues still remained as undesired degradation of the polyester backbone was observed during the attachment of certain drugs.

Herein, we describe the design evolution of three dendrimers that resulted in the creation of a new PEGylated dendrimer, which circumvented the synthetic and biological limitations uncovered in previous studies. We report a very efficient synthesis that combines the biocompatibility of bis-HMPA dendrimers with the robustness of polyamide dendrimers, yielding a hybrid scaffold capable of translation into clinical studies.

## MATERIALS AND METHODS

### Materials

Materials were used as obtained from commercial sources unless otherwise noted. Poly (ethylene glycol) was purchased from Laysan Biosciences Inc. Amino acid derivatives were purchased from Bachem. Dimethylformamide (DMF), pyridine, and dichloromethane (DCM) for syntheses were purged 1 h with nitrogen and further dried by passing them through commercially available push stills (Glass Contour). Solvents were removed under reduced pressure using a rotary evaporator or by vacuum pump evacuation. Compounds **2, 3, 4** (19), **6, 8, 9** (39), **10** (40), **15, 17, 18, 19** (41) were synthesized according to published procedures.

### Characterization

NMR spectra were recorded on Bruker AV 300, AVB 400, AVQ 400, or DRX 500 MHz instruments. Spectra were recorded in $CDCl_3$ or $D_2O$ solutions and were referenced to TMS or the solvent residual peak and taken at ambient temperature. Elemental analyses were performed at the UC Berkeley Mass Spectrometry Facility. MALDI-TOF MS was performed on a PerSeptive Biosystems Voyager-DE using the following matrices: *trans*-3-indoleacrylic acid (IAA) for *tert*-butyloxycarbonyl (Boc) protected dendrimers; or 2,5-dihyroxybenzoic acid (DHB) for amineterminated dendrimers. Samples were prepared by diluting dendrimer

solutions (~1 M) 40-fold in 100 mM matrix solutions in tetrahydrofuran and spotting 0.5 μL on the sample plate. Size exclusion chromatography (SEC) was performed using one of three systems:

*SEC System A:* a Waters 515 pump, a Waters 717 auto sampler, a Waters 996 Photodiode Array detector (210–600 nm), and a Waters 2414 differential refractive index (RI) detector. SEC was performed at 1.0 mL/min in a PLgel Mixed B (10 μm) and a PLgel Mixed C (5 μm) column (Polymer Laboratories, both 300 × 7.5 mm), in that order, using DMF with 0.2% LiBr as the mobile phase and linear PEO (4,200–478,000 MW) as the calibration standards. The columns were thermostated at 70 °C.

*SEC System B:* The same equipment as System A, but performed at 1.0 mL/min in two SDV Linear S (5 μm) columns (Polymer Standards Service, 300 × 8 mm) using DMF with 0.2% LiBr as the mobile phase.

*SEC System C:* A Waters Alliance separation module 2695 (sample compartment maintained at 37.0 ± 3.0 °C), a Waters 410 differential RI detector, a Waters 996 photodiode array detector (λ = 486 nm), and a Shodex OHpak SB-804 HQ SEC column. An isocratic flow rate of 0.7 mL/min was used with a mobile phase composed of 70%/30%/0.05% water/acetonitrile/formic acid.

Doxorubicin loading was quantified using a Lambda 35 UV-vis spectrometer (PerkinElmer, Wellesley, MA). Measurements were performed in sealed, standard 1-cm quartz cells in millipore water at room temperature.

## Animal and Tumor Models

All animal experiments were performed in compliance with National Institutes of Health guidelines for animal research under a protocol approved by the Committee on Animal Research at the University of California (San Francisco, CA) (UCSF). C26 colon carcinoma cells obtained from the UCSF cell culture facility were cultured in RPMI medium 1640 containing 10% FBS. Female BALB/c mice were obtained from Simonsen Laboratories, Inc. (Gilroy, CA).

## EA-$G_1$-Lys(Boc)$_8$ (22)

Pentaerythritol (353 mg, 2.6 mmol), BocLys(Boc)-ONp (5.500 g, 11.8 mmol) and 4-dimethylaminopyridine (DMAP) (125 mg, 1.0 mmol) were added to a 20 mL reaction vial. Under a nitrogen atmosphere, DMF (5.5 mL) and triethylamine (1.6 mL, 11.5 mmol) were added and the reaction stirred for 48 h. MALDI-TOF analysis confirmed the reaction had gone to completion. *N,N*-dimethylethylene diamine (300 μL, 4.1 mmol) was added to quench excess PNP esters. After 10 min, the mixture was diluted with ether (200 mL) and washed with three 100 mL portions of 1M NaOH, three 100 mL portions of 1M $NaHSO_4$, 100 mL DI water, and 100 mL of brine. The organic layer was dried over $Na_2SO_4$ and evaporated to dryness to give **22** (3.455 g, 93% yield) as a white foam. $^1$H NMR (400 MHz, $CDCl_3$): δ 1.26–1.49 (m, 88H), 1.58–1.83 (m, 8H), 3.09–3.11 (m, 8H), 4.08–4.18 (m, 12H), 4.80 (s, 4H), 5.3–5.6 (br d, 4H). $^{13}$C NMR (100 MHz, $CDCl_3$): δ 22.5, 28.3, 28.4, 29.6, 31.5, 39.9, 53.4, 62.2, 79.0, 79.8, 155.7, 156.1. Calc $[M]^+$ ($C_{69}H_{124}N_8O_{24}$) *m/z* = 1448.87. Found MALDI-TOF $[M+Na]^+$ *m/z* = 1470.0.

## EA-$G_1$-Lys($NH_3TFA$)$_8$ (22a)

Compound **22** (209 mg, 144 μmol) was dissolved in 1:1 trifluoroacetic acid (TFA): DCM for 1 h. Quantitative deprotection was confirmed by MALDI-TOF analysis. The solvents were removed under reduced pressure to give **22a** as a gummy solid in quantitative yield. $^1$H NMR

(400 MHz, MeOD): δ 1.40–1.60 (m, 8H), 1.67–1.75 (m, 8H), 1.87–2.10 (m, 8H), 2.99 (t, *J* = 8 Hz, 8H), 4.21 (t, *J* = 6 Hz, 4H), 4.40 (s, 8H). $^{13}$C NMR (100 MHz, MeOD): δ 21.8, 26.5, 29.5, 38.7, 42.5, 52.3, 62.9, 161.4, 161.7, 168.6. Calc $[M]^+$ ($C_{29}H_{60}N_8O_8$) *m/z* = 648.45. Found MALDI-TOF $[M+H]^+$ *m/z* = 649.6.

### EA-$G_1$-Lys(Glu(Bn)Boc)$_8$ (24)

Compound **22a** (89 mg, 63 μmol) and BocGlu(OBz)-ONp (290 mg, 632 μmol) were added to a 20 mL reaction vial. Under a nitrogen atmosphere, DMF (1 mL) and triethylamine (140 μL, 1.0 mmol) were added and the reaction was allowed to stir for 4 h. MALDI-TOF analysis showed a single peak corresponding to the fully functionalized dendrimer. *N*,*N*-dimethylethylene diamine (50 μl, 690 μmol) was added to quench excess PNP esters. The reaction was diluted with ethyl acetate (100 mL) and washed with three 50 mL portions of 1M $NaHSO_4$, three 50 mL portions of saturated $K_2CO_3$, 50 mL of DI water, and 50 mL brine. The organic layer was dried over $Na_2SO_4$ and evaporated to dryness to give **24** (171 mg, 87% yield) as a white foam. $^1$H NMR (400 MHz, MeOD): δ 1.41–1.56 (bm, 96H), 1.60–1.75 (m, 4H), 1.70–2.13 (m, 16H), 2.25–2.40 (m, 4H), 2.44–2.51 (m, 12H), 2.58–2.61 (m, 4H), 3.10–3.20 (m, 8H), 4.09–4.25 (m, 12H), 4.35–4.40 (m, 4H) 5.08–5.09 (2s, 16H), 7.28–7.38 (m, 40H). $^{13}$C NMR (100 MHz, MeOD): δ 23.8, 28.6, 31.5, 40.8, 44.6, 49.0, 54.4, 64.9, 163.4, 163.8, 170.7. Calc $[M]^+$ ($C_{165}H_{228}N_{16}O_{48}$) *m/z* = 3201.59. Found MALDI-TOF $[M+Na]^+$ *m/z* = 3223.3.

### EA-$G_1$-Lys(Glu(Bn)$NH_3$TFA)$_8$ (24a)

Compound **24** (100 mg, 31 μmol) was dissolved in 1:1 TFA:DCM for 1 h. Quantitative deprotection was confirmed by MALDI-TOF analysis. The solvents were removed under reduced pressure to give **24a** as a gummy solid in quantitative yield. $^1$H NMR (400 MHz, MeOD): δ 1.19–1.35 (m, 16H), 1.45–1.65 (m, 8H), 2.04–2.20 (m, 16H), 2.38–2.46 (m, 8H), 2.51–2.63 (m, 8H), 2.89–2.93 (m, 4H), 3.09–3.12 (m, 4H), 3.89–3.96 (m, 12H), 4.11 (t, *J* = 4.4 Hz, 4H), 4.30–4.33 (m, 4H), 4.80–5.00 (m, 16H), 7.17–7.26 (m, 40H). $^{13}$C NMR (100 MHz, MeOD): δ = 24.1, 27.7, 29.7, 30.3, 30.5, 31.6, 40.2, 53.5, 53.9, 54.1, 63.9, 67.8, 116.7, 119.6, 129.2, 129.3, 129.6, 137.3, 162.8, 163.2, 169.8, 170.3, 172.7, 173.6, 173.8. Calc $[M]^+$ ($C_{125}H_{164}N_{16}O_{32}$) *m/z* = 2402.73. Found MALDI-TOF $[M+Na]^+$ *m/z* = 2424.8.

### EA-$G_1$-Lys(Glu(Bn)PEO)$_8$ (25)

PNP-PEG carbonate (986 mg, 192 μmol) and **24a** (81 mg, 25 μmol $NH_3$) were added to a 20 mL reaction vial. Under a nitrogen atmosphere, DMF (3 mL) was added. After using a warm water bath to dissolve the starting material, triethylamine (120 μL, 0.863 mmol) was added. After stirring for 48 h (reaction monitored by SEC analysis), no further increase in the molecular weight was observed and the reaction was considered complete. Piperidine (50 μL, 0.506 mmol) was added to quench remaining PNP carbonate. After 1 h, acetic anhydride (400 μL, 4.24 mmol) was added to acylate any remaining primary amines on the dendrimer that had not reacted with the PNP-PEG carbonate. After stirring an additional hour, the reaction mixture was precipitated into ether (300 mL) and **25** (999 mg) was collected by filtration as a fluffy white solid. In some cases residual 5kDa PEG was observed after the PEGylation was considered complete. This could be removed by dialysis using 100,000 MWCO tubing against water for 24 hours. $^1$H NMR (500 MHz, $D_2O$): δ 1.20–1.80 (br m, 24H), 1.80–2.10 (br d, 16H), 2.35–2.55 (br s, 16H), 3.05–3.20 (br s, 8H), 3.38 (s, 24H), 3.40–3.90 (br m, ~3,900H), 4.00–4.40 (br m, 36H), 5.09–5.15 (br s, 16H), 7.25–7.40 (br m, 40H). DMF SEC: Mn: 32,000 Da, Mw: 35,000 Da, PDI: 1.09.

### EA-$G_1$-Lys(GluPEO)$_8$ (25a)

Compound **25** (402 mg, 10.1 μmol) was added to a 20 mL reaction vial and dissolved in MeOH (9 mL). Activated Pd/C (10 wt%, 50 mg) was added and the reaction put under hydrogen atmosphere. The reaction was stirred overnight, then filtered and solvent removed via rotary evaporation to give **25a** (387 mg) as a white solid. $^1$H NMR (500 MHz, $D_2O$): δ 1.20–1.80 (br m, 24H), 1.80–2.1 (br d, 16H), 2.40–2.51 (m, 16H), 3.15–3.25 (br s, 8H), 3.38 (s, 24H), 3.40–3.90 (br m, ~3,900H), 4.00–4.40 (br m, ~36H).

### EA-$G_1$-Lys(Glu(NNBoc)PEO)$_8$ (26)

Compound **25a** (710 mg, 142 μmol COOH), *t*-butyl carbazate (94 mg, 711 μmol), and DMAP (10 mg, 81 μmol) was added to a 20 mL reaction vial. Under a nitrogen atmosphere, DCM (8 mL) was added drop wise. The solution was cooled to 0 °C followed by the addition of 1-Ethyl-3-(3-dimethylaminopropyl)carbodiimide (EDC) (136 mg, 709 μmol). The reaction was allowed to warm to room temperature and stirred over night. The reaction was dialyzed against MeOH in 12kDa-14kDa MWCO dialysis with 3 solvent changes over 18 h. Concentration of the bag contents *in vacuo* gave **26** (660 mg) as a white solid. $^1$H NMR (500 MHz, $D_2O$): δ 1.30–1.60 (br m, 100H), 1.65–2.20 (br m, 20H), 2.30–2.45 (br s, 16H), 3.15–3.25 (br s, 8H), 3.38 (s, 24H), 3.50–3.90 (br m, ~3,900H), 4.00–4.45 (br m, 40H).

### EA-$G_1$-Lys(Glu(NNH$_3$TFA)PEO)$_8$ (26a)

Compound **26** (102 mg) was dissolved in 1:1 TFA: DCM for 1 h. The solvents were removed under reduced pressure to give 100 mg of **26a** as a gummy solid. $^1$H NMR (500 MHz, $D_2O$): δ 1.15–1.80 (br m, 24H), 1.85–2.00 (br m,16), 2.05–2.15 (br m, 16H), 2.15–2.25 (br m, 16H), 3.05–3.15 (br s,8H), 3.38 (s, 24H), 3.50–3.90 (br m, ~3,900H), 4.00–4.45 (br m, 40H).

### EA-$G_1$-Lys(Glu(NNDox)PEO)$_8$ (27)

Compound **26a** (72 mg, 14 μmol NNBoc) and doxorubicin (50 mg, 92 μmol) were added to a 20 mL reaction vial and were dissolved in MeOH (3 mL), pyridine (100 μL), and acetic acid (100 μL). The reaction was purged with nitrogen and stirred at 60 °C in the dark for 18 h. The reaction mixture was loaded directly onto a Sephadex LH-20 column and eluted with methanol. The first dark red band was collected and the solvent removed by rotary evaporation. The solid material was further purified using a Biorad PD-10 column with water as the eluent. After lyophilization 67.2 mg of red powder remained. The Dox loading was quantified using the absorbance at 486 nm (ε = 11,500) (42) to be 9.6 wt %, or 88% of the maximum theoretical loading.

### Polymer Degradation Study

Compound **26** (20 mg) was dissolved in 1.5 mL of 1X PBS buffer and incubated at 37 °C. At t = 0, 1, 2, 3, 6, 15, 20 days, 100 μL aliquots were taken out and immediately frozen followed by lyophilization. At the end of the experiment, each sample was dissolved in 0.5 mL DMF from the System A mobile phase, filtered though a 0.2 μm PVTF filter and measured by the RI detector on system A.

### Hydrolysis of Dox from Compound 27 at pH 7.4 and pH 5

Drug release rates were determined by a modified published procedure (43). Compound **27** was dissolved in either 1X PBS or pH 5 acetate buffer (30 mM with 70 mM $NaNO_3$), at 1 mg/mL. Buffers were preheated to 37 °C before dissolving polymer and maintained at this temperature throughout the experiment. At each time point, 25 μL was injected onto SEC system C for analysis.

### Cytotoxicity Studies in Cells

The cytotoxicities of free Dox, **26**, and **27** were determined by using the MTT assay with C26 cells. Cells were seeded onto a 96-well plate at a density of $5.0 \times 10^3$ cells per well in 100 μL of medium and incubated overnight (37 °C, 5% $CO_2$, and 80% humidity). An additional 100 μL of new medium (RPMI medium 1640, 10% FBS, 1% penicillin-streptomycin, 1% Glutamax) containing varying concentrations of Dox, **26**, or **27** were added to each well. After incubation for 72 h, 40 μL of media containing thiazolyl blue tetrazolium bromide (5 mg/mL) was added. The cells were incubated for 3 h, after which time the medium was carefully removed. To the resulting purple crystals was added 200 μL of DMSO and 25 μL of pH 10.5 glycine buffer (0.1 M glycine/0.1 M NaCl). Optical densities were measure at 570 nm by a SpectraMAX 190 microplate reader (Molecular Devices, Sunnyvale, CA). Optical densities measured for wells containing cells that received neither dendrimer nor drug were considered to represent 100% viability. $IC_{50}$ values were obtained from sigmoidal fits of the data using Origin 7 SR4 8.0552 software (OriginLab, Northampton, MA).

### Biodistribution Study in Xenograph Mice

Six to eight week old female Balb/C mice were injected in the right hind flank with $3 \times 10^5$ C26 cells. Twelve days after tumor inoculation, mice were randomized into two groups. Mice were injected by means of the tail vein either with Doxil™ (8 mg Dox eq/kg; 3 mice) or with **27** (8 mg Dox eq/kg; 6 mice) in ~200 μL of PBS. Blood was collected from half of the mice injected with polymer by submandibular bleeds 60 and 1440 min after dosing (data not shown); after 2880 min, the three mice were sacrificed. The remaining six mice were sacrificed at 1 wk postinjection. The blood (collected by heart puncture), heart, liver, spleen, kidney, muscle, and tumor were collected for analysis. Each organ was weighed and 200–300 mg of the collected organs were homogenized with zirconium beads and 1 mL acidified isopropyl alcohol (0.075 M HCl, 90% IPA). The samples then incubated at 4 °C for 24 h. Serum was collected using Microtainer serum separator vials and processed in the same manner as the organs. The samples were frozen in a −80 °C freezer until measurements could be made. At measurement time, samples were thawed, briefly vortexed, and centrifuged for 3 min at 8,000 rpm. Then, 80 μL of supernatant was combined with 920 μL of acidified IPA for fluorescence measurements. Dox fluorescence (excitation 490 nm; emission 590 nm) was measured on a PTI fluorimeter (Birmingham, NJ). Calibration curves were made from organ samples collected from an untreated mouse.

### Chemotherapy Experiments

While under anesthesia, female Balb/C mice were shaved, and C26 cells ($3 \times 10^5$ cells in 50 μL) were injected subcutaneously in the right hand flank. At eight days post-tumor implantation, mice were randomly distributed into treatment groups of 10 animals. Mice were injected by means of the tail vein with Doxil™ (20 mg Dox/kg) or **27** (10, 15, and 20 mg Dox/kg) in approximately 200 μL of solution. Mice were weighed and tumors measured every other day. The tumor volume was estimated by measuring the tumor volume in three dimension with calipers and calculated using the formula tumor volume = length × width × height. Mice were removed from the study when (i) a mouse lost 15% of its initial weight, (ii) any tumor dimension was > 20 mm, or (iii) the mouse was found dead. The mice were followed until day 60 post-tumor inoculation. Statistical analysis was performed as previously described (41) using MedCalc 8.2.1.0 for Windows (MedCalc Software, Mariakerke, Belgium). The tumor growth delay was calculated based upon a designated tumor volume of 400 $mm^3$.

# RESULTS AND DISCUSSION

## Exploring Polyester-Core Dendrimers

Polyester dendrimers based on bis(HMPA) monomer units are an attractive scaffold for biological applications because they are non-immunogenic, biodegradable, and non-toxic (36). Scheme 1 outlines the synthesis of a core-functionalized PEGylated dendrimer we have developed earlier (39). Briefly, the tetrafunctional pentaerythritol core **1** was modified with a benzylidene-protected bis(HMPA) monomer **2** to afford the first generation dendrimer **3**. After removal of the protecting groups via hydrogenolysis, the eight peripheral hydroxyl groups were functionalized with orthogonally protected aspartic acid to give **6**. Subsequent deprotection of the amino groups of **6** followed by PEGylation with the 5 kDa PEG electrophiles gave dendrimer **8**. Removal of the benzyl ester protecting groups of **8** via hydrogenolysis afforded dendrimer **9** with eight carboxylic acids moieties available for potential drug attachment. However, early attempts at the functionalization of this dendrimer with *t*-butyl carbazate or glutamic acid derivative **10** were unsuccessful as degradation of the dendrimer was observed during this reaction.

In order to gain insight into the degradation pathway, we prepared the dendrimer probe **11** and attempted to functionalize its aspartic acid chain-ends with *t*-butyl carbazate. Probe molecule **11** was selected instead of PEGylated dendrimer **9** as progress of its reaction could be more easily monitored by MALDI-TOF since it does not contain PEG chains (Figure 1). As a result of a degradation side reaction, only a small amount of the target product was formed, leading to the appearance of lower molecular weight products with molecular weights that decreased in increments of 329 amu, likely as a result of intramolecular cyclization reactions as proposed in Figure 1. This type of cyclization reaction on benzyl ester-protected aspartic acid residues is documented in the peptide literature and additives have been developed to suppress such reactions (44). For example, pentachlorophenol (PCP) has been used to decrease the production of the aminosuccinyl by-product by inhibiting amide deprotonation. Under these buffered conditions, the primary amines are still available to react with *p*-nitrophenyl (PNP) carbonates and other electrophiles. The use of PCP as an additive proved beneficial in our hands as it allowed the functionalization of the carboxylic acid side chains of dendrimer **9** with protected nucleophile **10** to give dendrimer **12** (Scheme 2). Finally, doxorubicin hydrazone conjugate **14** was obtained after removal of the Boc groups from the hydrazide linkers in **12** and condensation of the resulting amines with the ketone group of doxorubicin **13**. In order to determine how rapidly this polyester architecture breaks down under physiological conditions, **12** was incubated in PBS buffer at 37 °C and the evolution of its molecular weight with time was monitored by SEC. This revealed that the α-amino esters located did not survive long enough for use of **12** *in vivo* as significant degradation was observed after only 10 hours. For this reason, we began exploring alternative dendrimer scaffolds based on more robust polyamide cores.

## Exploring Polylysine-Core Dendrimers

In contrast to polyester dendrimers, polyamide dendrimers are less susceptible to hydrolysis, but this increased stability may hamper their break down *in vivo*. Recently, Fox *et al.* functionalized a PEGylated polylysine with camptothecin and observed complete tumor remission in transgenic mice with HT-29 human colon carcinoma (41). While the degradation of amide bonds in linear peptides *in vivo* is well established, the fate of branched, acylated, and PEGylated polyamide dendrimers is less certain as proteases may not be able to access amide bonds near the core of the structure. However, even slow or incomplete degradation of the carrier may be permissible for drug delivery applications if the by-products are non-toxic and small in size (45,46). In order to apply the polylysine carrier used by Fox (41) to the delivery of doxorubicin, dendrimer **18** with a protected hydrazide had to be prepared.

Lysine dendrimer **15**, first described by Denkewalter (47) in 1982 was used as the starting material. Its peripheral amines were acylated with PNP-Asp(Bn)Boc to afford dendrimer **17** (Scheme 3). It is worth noting that the PCP additive was also needed when attaching aspartic acid to the $G_2$ lysine periphery. Otherwise, a 5-membered amino succinyl byproduct can form via amidolysis of the benzyl ester protected side chain. Deprotection of the amino groups of the aspartate termini and PEGylation with PEG-*p*-nitrophenyl carbonate afforded **18**. Unfortunately, the coupling of t-butyl carbazate to the deprotected side chain carboxylic acid terminal moieties **(19)** led to the appearance of degradation byproducts such as **20** (Figure 2). Monitoring of the reaction by size exclusion chromatography (Figure 2) showed the formation of lower molecular weight by products - presumably formed as a result of attack of the hydrazide nitrogens onto the carbamate linkers to PEG, thus forming a six-membered cyclic by-product and releasing PEG.

This side reaction could be circumvented in two ways (see Supporting Information): (i) replacement of the carbamate in **18** with a more stable amide linkage by using carboxymethyl terminated PEG instead of a PNP carbamate; or (ii) use of a glutamic acid spacer between the nucleophilic hydrazides and the relatively labile carbamate linkages to PEG. The latter route requires more synthetic operations, but has the added benefit of doubling the number of hydrazides through which drug molecules can be attached. Overall, while feasible, this route did not fully meet our criteria for an optimized dendritic drug carrier.

## Exploring Hybrid Ester-Amide-Core Dendrimers

The important lessons learned from the synthesis of both the polyester and polyamide carriers ultimately led us to consider a hybrid approach that combines their separate virtues in one scaffold. It appears that the combination of a hydrolytically degradable ester core and a more chemically resistant amide periphery might be ideal for the construction of PEGylated drug conjugates. Furthermore, the early designs we tested (*vide supra*) also underscored the importance of avoiding the positioning nucleophilic sites at a 5- or 6-atom distance from potential leaving groups (43). Hybrid dendrimer **24** (Scheme 4), representing such an architecture was obtained in three simple steps and 81% overall yield without any chromatographic purification.

Synthesis of the hybrid carrier began by treatment of pentaerythritol **1** with the *p*-nitrophenyl ester of lysine **21** (Scheme 4). The amine protecting groups of the resulting dendrimer **22** were then removed and the molecule was provided with “differentiated end functionalities” by reacting each of its eight primary amino groups with orthogonally protected PNP-glutamic acid **23**. Glutamic acid was selected over aspartic acid for the following reasons: (i) pentachlorophenol was no longer needed to prevent amidolysis of the benzyl ester group, since formation of the 6-membered amino succinyl byproduct was not observed; and (ii) *t*-butyl carbazate could be attached directly to the glutamic acid side chain without any degradation as cyclization of the acyl hydrazide onto the carbamate to form a 7-membered ring was not an issue. Eight 5 kDa PEG chain were then installed on the dendrimer periphery via a carbamate linkage. This was accomplished by quantitative removal of the Boc protecting groups and subsequent PEGylation with one equivalent (per amine) of PNP-PEG (Scheme 4). The PEGylation reaction was extended over two days, at which time, piperidine was added to quench any unreacted PNP-PEG, and then acetic anhydride was added to acylate any remaining primary amines on the dendrimer scaffold. The resulting PEGylated dendrimer **25** was purified via precipitation into ether to give a polymer with MW ~40,000 Da and PDI < 1.1, with an average particle size of 12 nm as determined by dynamic light scattering (DLS). Finally, residual linear PEG could be removed by dialysis using 100,000 MW cut-off dialysis tubing in water.

The benzyl ester protected side chains of the glutamic acid moieties in **25** were removed via hydrogenolysis, and the resultant carboxylic acids were treated with *t*-butyl carbazate and 1-ethyl-3-(3-dimethylaminopropyl)carbodiimide (EDC) to give dendrimer **26** with eight protected hydrazides available for drug attachment. Finally, target drug conjugate **27** was successfully obtained from the protected precursor **26** by removal of the Boc groups and subsequent condensation with doxorubicin in 5% pyridine/acetic acid solution of methanol at 60 °C.

The degradation profile of the ester-amide dendrimer hybrid was evaluated under physiological conditions. Polymer **26** was incubated at 37 °C in phosphate buffer at physiological pH and the molecular weight was monitored over 20 days by size exclusion chromatography (Figure 3a). As expected, the polymer degraded into 10 kDa and 5 kDa fragments as a result of the slow hydrolysis of both ester and carbamate moieties. Given that the threshold for renal clearance for linear polymers is estimated to be near 45,000 Daltons (48), cleavage of the 40,000 Dalton branched polymer following delivery of its payload contributes to prevent its long-term accumulation. The observed degradation profile is promising as it suggests that hybrid dendrimer **26** is sufficiently stable to allow for selective tumor uptake, yet can be eventually broken down and cleared (9). It is also noteworthy that the drug is attached to a narrow population of polymeric material and that no significant amount of free drug is present as confirmed by the absence of a peak corresponding to free drug at 590 nm in the UV-vis trace of the conjugate (Figure 3b).

Carrier drug loading was determined via UV-vis spectroscopy and could be varied from 6–10 wt/wt% depending on how many equivalents of doxorubicin were used in the loading step. This correlates to 55–92% of the theoretical maximum doxorubicin loading for a ~40 kDa polymer with 8 sites for drug attachment. Doxorubicin was chosen for attachment because it is a well-established and highly effective chemotherapeutic agent (49) that can benefit from conjugation to a carrier to decrease its innate cardiotoxicity. It is important to note that a variety of drugs, prodrugs, or other biological agents may potentially be attached to dendritic carriers based on **25** through its latent carboxylic acid side chains. The pH-dependence for the rate of hydrolysis of the hydrazone bond we formed is well studied (43,50,51), and we could confirm that the drug would be selectively released under acidic conditions similar to those found in the lysosome (43). At pH 7.4, less than 5% of drug was released over 48 hours while the half-life of hydrolysis at pH 5 was 22 hours.

### *In Vitro* Toxicity of Ester-Amide Dendrimer

The *in vitro* cytotoxicity tests showed that **26** remained non-toxic toward C26 cells at a concentration of 5 mg/mL. When Dox was conjugated to the carrier, a ten-fold decrease in toxicity was observed over the free Dox ($IC_{50(\mathbf{27})}$ = 529.6 +/− 3.8 nM; $IC_{50(Dox)}$ = 52.4 +/− 12.7 nM). The decrease in toxicity may be attributed to the slower rate of uptake of the ester-amide carrier compared to free Dox and the slow hydrolysis of the drug from the carrier.

### Biodistribution in Tumored Mice

The biodistribution of the ester-amide dendrimer was determined in C26 tumored female Balb/C mice Figure. Mice were injected with 8 mg Dox eq/kg, formulated as Doxil™ or **27**. After 48 h, Dox accumulation within the tumor was 5.5 ± 0.7 % ID/g of tissue (compared to vital organs, $p < 0.001$), whereas, accumulation in the vital organs was less than 2 % ID/g of tissue. This result is comparable to the levels of accumulation we have previously observed for related macromolecules (36,39). Furthermore, we were pleased to find a measurable level of Dox still remained within the tumor tissue (compared to vital organs, $p < 0.05$) after one week with little accumulation within the vital organs. Mice injected with **27** or Doxil™ had comparable tumor accumulation after one week, 3.7 ± 0.51 % ID/g of tissue and 5.27 ± 5.19 % ID/g of tissue

respectively. The ester-amide dendrimer showed lower accumulation within the spleen than Doxil™. Lowering Dox accumulation in the vital organs is important for reducing systemic toxicity, while uptake by tumor tissue must be maintained to promote treatment efficacy.

### Chemotherapy Study in Tumored Mice

A dose-response experiment was performed in C26 tumored Balb/C mice; four treatment groups were investigated, Doxil™ (20 mg Dox/kg) and **27** (10, 15, and 20 mg Dox/kg). Dose-dependent survival was observed and all three groups treated with **27** showed significant tumor growth delay (TGD) and prolonged survival (Table 1, Figure 5). Mice treated with **27** at 20 mg Dox/kg had 9 out of 10 mice tumor free at the end of the study (day 60), with TGD of 229% ($p < 0.0001$) and median survival time of 60 days. For **27** administered at 15 mg Dox/kg and 10 mg Dox/kg, the treatment groups had 175% ($p < 0.0001$), and 74% TGD ($p < 0.0001$) and a median survival time of 60, and 33 days respectively. Doxil™ had 8 out of 10 mice alive at day 60, but the two deaths appeared to be due to treatment-related toxicity. Weight loss due to treatment toxicity was on average not severe, with a mean weight loss of 6.4% for Doxil™ and 4.3% for **27** (20 mg Dox/kg). This result is comparable to the chemotherapy experiment with the asymmetrically PEGylated dendrimer vs. Doxil™, both administered at 20 mg Dox/kg (17). In this earlier study, there was complete tumor regression with the asymmetrically PEGylated dendrimer carrier with a single toxic death observed in the parallel Doxil™ experiment. Therefore both the current and the earlier studies confirm that Dox-loaded PEGylated dendrimer carriers are as effective as Doxil™ against the C26 tumor model. The ester-amide dendrimer **27** may exhibit less toxicity than Doxil™ at equivalent Dox dosages and its biodegradability, streamlined synthesis, and facile storage as a dry powder offer significant advantages over existing treatments.

## CONCLUSION

In conclusion, the attractive features of polyester and polyamide dendrimers have been combined to form a robust yet degradable polyvalent macromolecular scaffold that can be prepared in a scalable fashion. The final drug loaded dendrimer is made entirely from commercial starting materials in nine high-yielding steps, four of which are near quantitative deprotection steps. No chromatographic steps are required during the dendrimer preparation. This scaffold will be studied with additional tumor models and drugs as it shows promise as a clinically relevant delivery vehicle.

## Supplementary Material

Refer to Web version on PubMed Central for supplementary material.

## Acknowledgments

Financial support of this research by the National Institutes of Health (RO1 EB 002047) is gratefully acknowledged. We thank Dr. Megan Fox for insightful discussions.

## LITERATURE CITED

1. Kopecek J. Soluble Biomedical Polymers. Polymers in Medicine 1977;7:191–221. [PubMed: 593972]
2. Bader H, Ringsdorf H, Schmidt B. Water-soluble Polymers in Medicine. Angew. Makromol. Chem 1984;123:457–485.
3. Seymour LW. Passive Tumor Targeting of Soluble Macromolecules and Drug Conjugates. Crit. Rev. Ther. Drug 1992;9:135–187.

4. Matsumura Y, Maeda H. A New Concept for Macromolecular Therapeutics in Cancer-Chemotherapy - Mechanism of Tumoritropic Accumulation of Proteins and the Antitumor Agent Smancs. Cancer Res 1986;46:6387–6392. [PubMed: 2946403]
5. Liu S, Maheshwari R, Kiick KL. Polymer-Based Therapeutics. Macromolecules 2009;42:3–13.
6. Kataoka K, Harada A, Nagasaki Y. Block copolymer micelles for drug delivery: design, characterization and biological significance. Adv. Drug Delivery Rev 2001;47:113–131.
7. Guo X, Szoka FC. Chemical approaches to triggerable lipid vesicles for drug and gene delivery. Accounts Chem. Res 2003;36:335–341.
8. Christian DA, Cai S, Bowen DM, Kim Y, Pajerowski JD, Discher DE. Polymersome carriers: From self-assembly to siRNA and protein therapeutics. Eur. J. Pharm. Biopharm 2009;71:463–474. [PubMed: 18977437]
9. Fox ME, Szoka FC, Fréchet JMJ. Soluble Polymer Carriers for the Treatment of Cancer: The Importance of Molecular Architecture. Accounts Chem. Res 2009;42:1141–1151.
10. Li MH, Keller P. Stimuli-responsive polymer vesicles. Soft Matter 2009;5:927–937.
11. Green JJ, Langer R, Anderson DG. A combinatorial polymer library approach yields insight into nonviral gene delivery. Accounts Chem. Res 2008;41:749–759.
12. Haag R, Kratz F. Polymer therapeutics: Concepts and applications. Angew. Chem. Int. Edit 2006;45:1198–1215.
13. Peer D, Karp JM, Hong S, Farokhzad OC, Margalit R, Langer R. Nanocarriers as an emerging platform for cancer therapy. Nat. Nanotechnol 2007;2:751–760. [PubMed: 18654426]
14. Medina SH, El-Sayed MEH. Dendrimers as Carriers for Delivery of Chemotherapeutic Agents. Chem. Rev 2009;109:3141–3157. [PubMed: 19534493]
15. Gillies ER, Fréchet JMJ. Dendrimers and dendritic polymers in drug delivery. Drug Discov. Today 2005;10:35–43. [PubMed: 15676297]
16. Lee CC, MacKay JA, Fréchet JMJ, Szoka FC. Designing dendrimers for biological applications. Nat. Biotechnol 2005;23:1517–1526. [PubMed: 16333296]
17. Lee CC, Gillies ER, Fox ME, Guillaudeu SJ, Fréchet JMJ, Dy EE, Szoka FC. A single dose of doxorubicin-functionalized bow-tie dendrimer cures mice bearing C-26 colon carcinomas. P. Natl. Acad. Sci. USA 2006;103:16649–16654.
18. De Jesus OLP, Ihre HR, Gagne L, Fréchet JMJ, Szoka FC. Polyester dendritic systems for drug delivery applications: In vitro and in vivo evaluation. Bioconjugate Chem 2002;13:453–461.
19. Parrott MC, Marchington EB, Valliant JF, Adronov A. Synthesis and properties of carborane-functionalized aliphatic polyester dendrimers. J. Am. Chem. Soc 2005;127:12081–12089. [PubMed: 16117549]
20. Bellis E, Hajba L, Kovacs B, Sandor K, Kollar L, Kokotos G. Three generations of alpha, gamma-diaminobutyric acid modified poly(propyleneimine) dendrimers and their cisplatin-type platinum complexes. J. Biochem. Bioph. Meth 2006;69:151–161.
21. Krishna TR, Jain S, Tatu US, Jayaraman N. Synthesis and biological evaluation of 3-amino-propan-1-ol based poly(ether imine) dendrimers. Tetrahedron 2005;61:4281–4288.
22. Chen HT, Neerman MF, Parrish AR, Simanek EE. Cytotoxicity, hemolysis, and acute in vivo toxicity of dendrimers based on melamine, candidate vehicles for drug delivery. J. Am. Chem. Soc 2004;126:10044–10048. [PubMed: 15303879]
23. Lim JD, Simanek EE. Synthesis of water-soluble dendrimers based on melamine bearing 16 paclitaxel groups. Org. Lett 2008;10:201–204. [PubMed: 18088131]
24. Lim J, Guo Y, Rostollan CL, Stanfield J, Hsieh JT, Sun XK, Simanek EE. The role of the size and number of polyethylene glycol chains in the biodistribution and tumor localization of triazine dendrimers. Mol. Pharmaceut 2008;5:540–547.
25. Esfand R, Tomalia D. Poly(amidoamine) (PAMAM) dendrimers: from biomimicry to drug delivery and biomedical applications. Drug Discov. Today 2001;6:427–436. [PubMed: 11301287]
26. Khandare JJ, Jayant S, Singh A, Chandna P, Wang Y, Vorsa N, Minko T. Dendrimer versus linear conjugate: Influence of polymeric architecture on the delivery and anticancer effect of paclitaxel. Bioconjugate Chem 2006;17:1464–1472.

27. Kono K, Kojima C, Hayashi N, Nishisaka E, Kiura K, Wataral S, Harada A. Preparation and cytotoxic activity of poly(ethylene glycol)-modified poly(amidoamine) dendrimers bearing adriamycin. Biomaterials 2008;29:1664–1675. [PubMed: 18194811]
28. Bhadra D, Bhadra S, Jain S, Jain NK. A PEGylated dendritic nanoparticulate carrier of fluorouracil. Int. J. Pharm 2003;257:111–124. [PubMed: 12711167]
29. Patri AK, Myc A, Beals J, Thomas TP, Bander NH, Baker JR. Synthesis and in vitro testing of J591 antibody-dendrimer conjugates for targeted prostate cancer therapy. Bioconjugate Chem 2004;15:1174–1181.
30. Malik N, Evagorou EG, Duncan R. Dendrimer-platinate: a novel approach to cancer chemotherapy. Anti-Cancer Drugs 1999;10:767–776. [PubMed: 10573209]
31. Kaminskas LM, Kelly BD, McLeod VM, Boyd BJ, Krippner GY, Williams ED, Porter CJH. Pharmacokinetics and Tumor Disposition of PEGylated, Methotrexate Conjugated Poly-L-lysine Dendrimers. Mol. Pharmaceut 2009;6:1190–1204.
32. Kaneshiro TL, Wang X, Lu ZR. Synthesis, characterization, and gene delivery of Poly-L-lysine octa (3-aminopropyl)silsesquioxane dendrimers: nanoglobular drug carriers with precisely defined molecular Architectures. Mol. Pharmaceut 2007;4:759–768.
33. Okuda T, Kawakami S, Akimoto N, Niidome T, Yamashita F, Hashida M. PEGylated lysine dendrimers for tumor-selective targeting after intravenous injection in tumor-bearing mice. J. Control. Release 2006;116:330–336. [PubMed: 17118476]
34. Grinstaff MW. Biodendrimers: New polymeric biomaterials for tissues engineering. Chem.-Eur. J 2002;8:2838–2846.
35. Malik N, Wiwattanapatapee R, Klopsch R, Lorenz K, Frey H, Weener JW, Meijer EW, Paulus W, Duncan R. Dendrimers: Relationship between structure and biocompatibility in vitro, and preliminary studies on the biodistribution of I-125-labelled polyamidoamine dendrimers in vivo (vol 65, pg 133, 2000). J. Control. Release 2000;68:299–302.
36. Gillies ER, Dy E, Fréchet JMJ, Szoka FC. Biological evaluation of polyester dendrimer: Poly(ethylene oxide) "Bow-Tie" hybrids with tunable molecular weight and architecture. Mol. Pharmaceut 2005;2:129–138.
37. Gillies ER, Fréchet JMJ. Designing macromolecules for therapeutic applications: Polyester dendrimer-poly(ethylene oxide) "bow-tie" hybrids with tunable molecular weight and architecture. J. Am. Chem. Soc 2002;124:14137–14146. [PubMed: 12440912]
38. Goodwin, aP; Lam, SS.; Fréchet, JMJ. Rapid, efficient synthesis of heterobifunctional biodegradable dendrimers. J. Am. Chem. Soc 2007;129:6994–6995. [PubMed: 17489595]
39. Guillaudeu SJ, Fox ME, Haidar YM, Dy EE, Szoka FC, Fréchet JMJ. PEGylated dendrimers with core functionality for biological applications. Bioconjugate Chem 2008;19:461–469.
40. King HD, Yurgaitis D, Willner D, Firestone RA, Yang MB, Lasch SJ, Hellstrom KE, Trail PA. Monoclonal antibody conjugates of doxorubicin prepared with branched linkers: A novel method for increasing the potency of doxorubicin immunoconjugates. Bioconjugate Chem 1999;10:279–288.
41. Fox ME, Guillaudeu S, Fréchet JMJ, Jerger K, Macaraeg N, Szoka FC. Synthesis and In Vivo Antitumor Efficacy of PEGylated Poly(L-lysine) Dendrimer-Camptothecin Conjugates. Mol. Pharmaceut 2009;6:1562–1572.
42. Gabbay EJ, Grier D, Fingerle RE, Reimer R, Levy R, Pearce SW, Wilson WD. Interaction Specificity of Anthracyclines with Deoxyribonucleic-Acid. Biochemistry 1976;15:2062–2070. [PubMed: 776212]
43. Lee CC, Cramer AT, Szoka FC, Fréchet JMJ. An intramolecular cyclization reaction is responsible for the in vivo inefficacy and apparent pH insensitive hydrolysis kinetics of hydrazone carboxylate derivatives of doxorubicin. Bioconjugate Chem 2006;17:1364–1368.
44. Martinez J, Bodanszky M. Side Reactions in Peptide-Synthesis.9. Suppression of the Formation of Aminosuccinyl Peptides with Additives. Int. J. Pept. Prot. Res 1978;12:277–283.
45. Tekade RK, Kumar PV, Jain NK. Dendrimers in Oncology: An Expanding Horizon. Chem. Rev 2009;109:49–87. [PubMed: 19099452]
46. Kaminskas LM, Boyd BJ, Karellas P, Krippner GY, Lessene R, Kelly B, Porter CJH. The impact of molecular weight and PEG chain length on the systemic pharmacokinetics of PEGylated poly L-lysine dendrimers. Mol. Pharmaceut 2008;5:449–463.

47. Denkewalter. U.S. Patent. 4,360,646. 1982.

48. Seymour LW, Duncan R, Strohalm J, Kopecek J. Effect of Molecular-Weight (Mbarw) of N-(2-Hydroxypropyl)Methacrylamide Copolymers on Body Distribution and Rate of Excretion after Subcutaneous, Intraperitoneal, and Intravenous Administration to Rats. J. Biomed. Mater. Res 1987;21:1341–1358. [PubMed: 3680316]

49. Kratz F, Warnecke A, Schmid B, Chung DE, Gitzel M. Prodrugs of anthracyclines in cancer chemotherapy. Curr. Med. Chem 2006;13:477–523. [PubMed: 16515518]

50. Bae Y, Nishiyama N, Fukushima S, Koyama H, Yasuhiro M, Kataoka K. Preparation and biological characterization of polymeric micelle drug carriers with intracellular pH-triggered drug release property: Tumor permeability, controlled subcellular drug distribution, and enhanced in vivo antitumor efficacy. Bioconjugate Chem 2005;16:122–130.

51. Ulbrich K, Etrych T, Chytil P, Jelinkova M, Rihova B. HPMA copolymers with pH-controlled release of doxorubicin - In vitro cytotoxicity and in vivo antitumor activity. J. Control. Release 2003;87:33–47. [PubMed: 12618021]

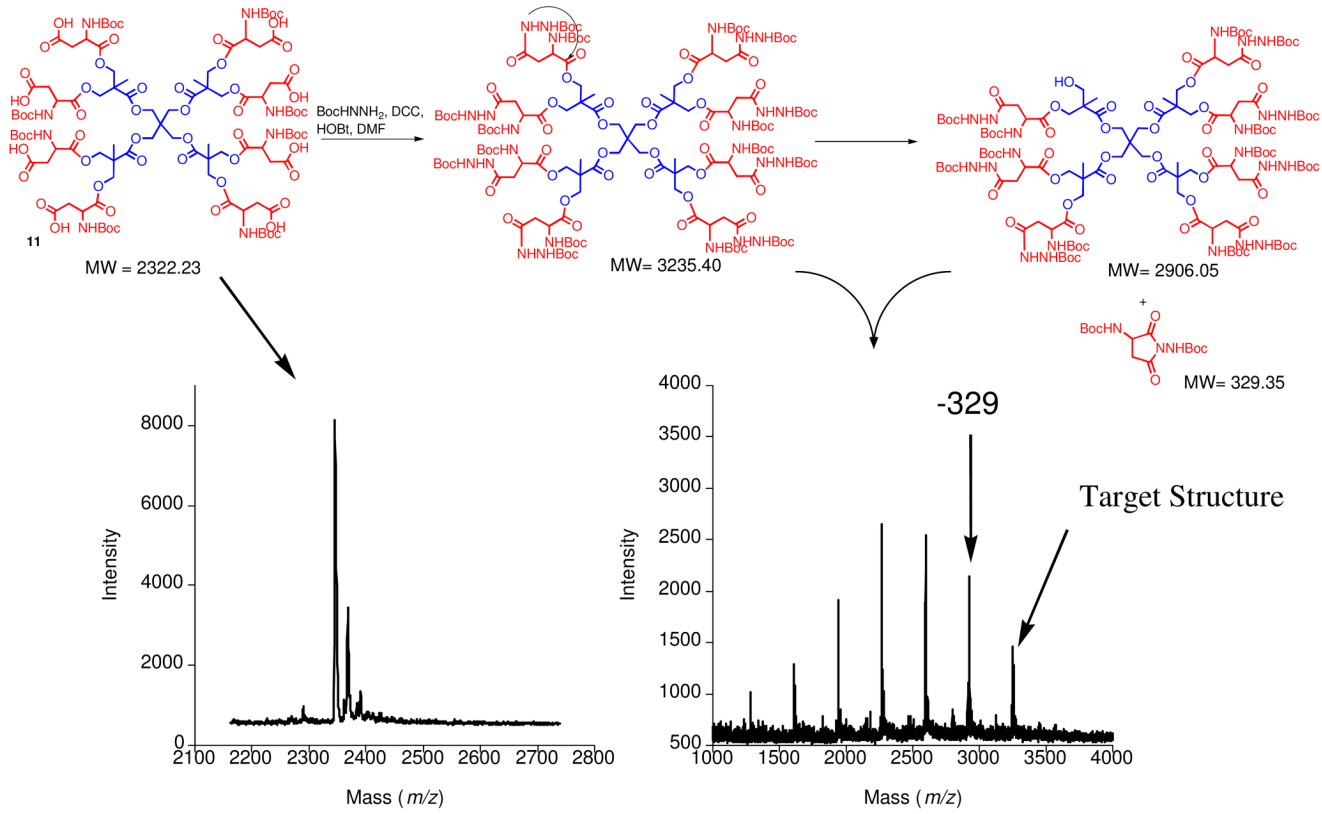


**Figure 1.**
Proposed degradation pathway for polyester dendrimer.

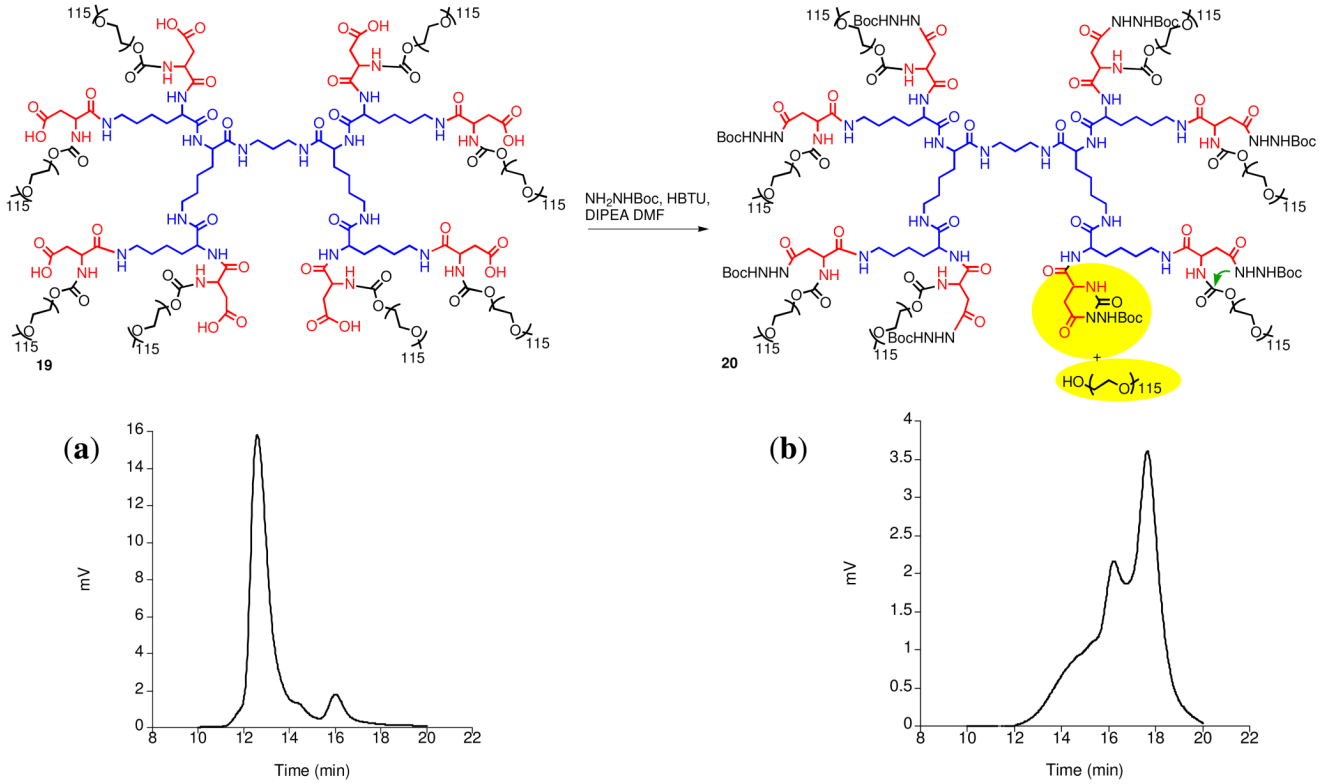


**Figure 2.**
PEGylated polylysine degradation: (a) SEC of compound **19**, (b) SEC of reaction mixture with by-product **20**.

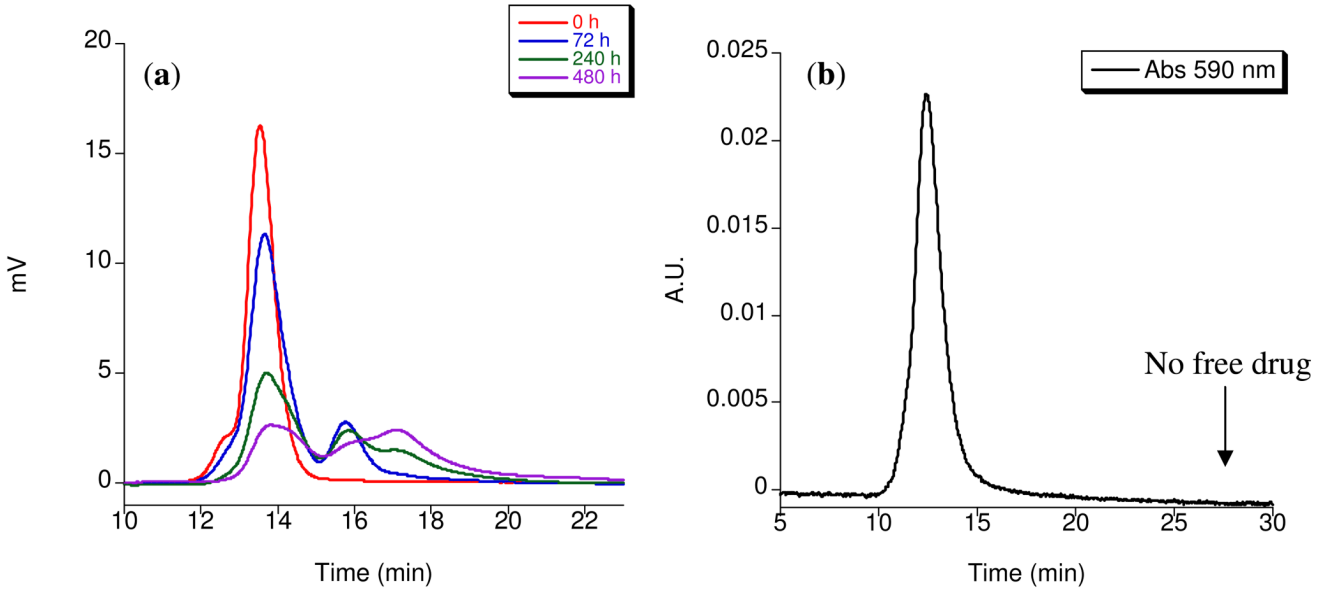


**Figure 3.**
a) Size exclusion chromatographs of **26** in pH 7.4 PBS buffer at 37 °C. b) UV-vis size exclusion chromatograph of **27** at 590 nm.

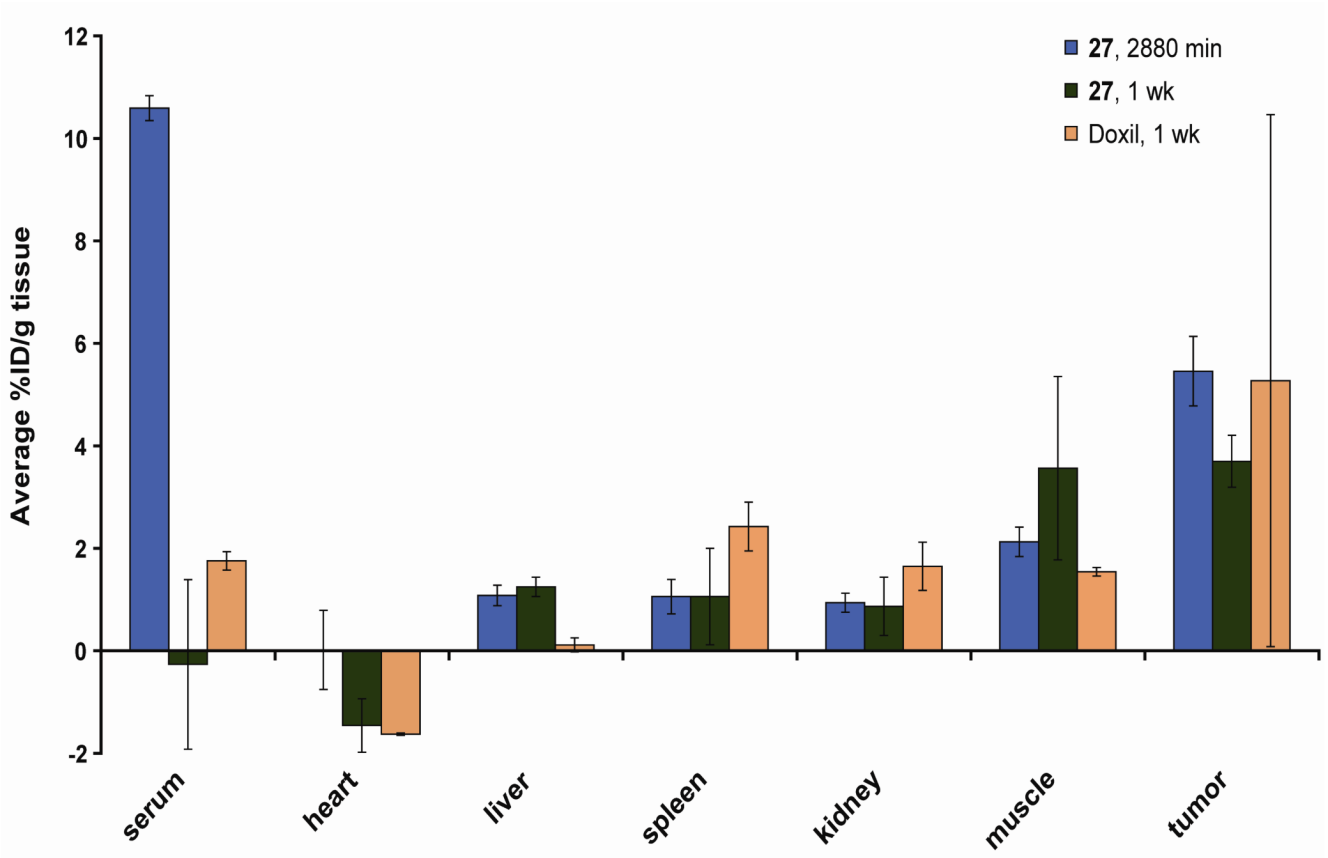


**Figure 4.**
48 hour and 1 week biodistribution of **27** and 1 week biodistribution of Doxil™ in mice with s.c. C26 colon carcinoma.

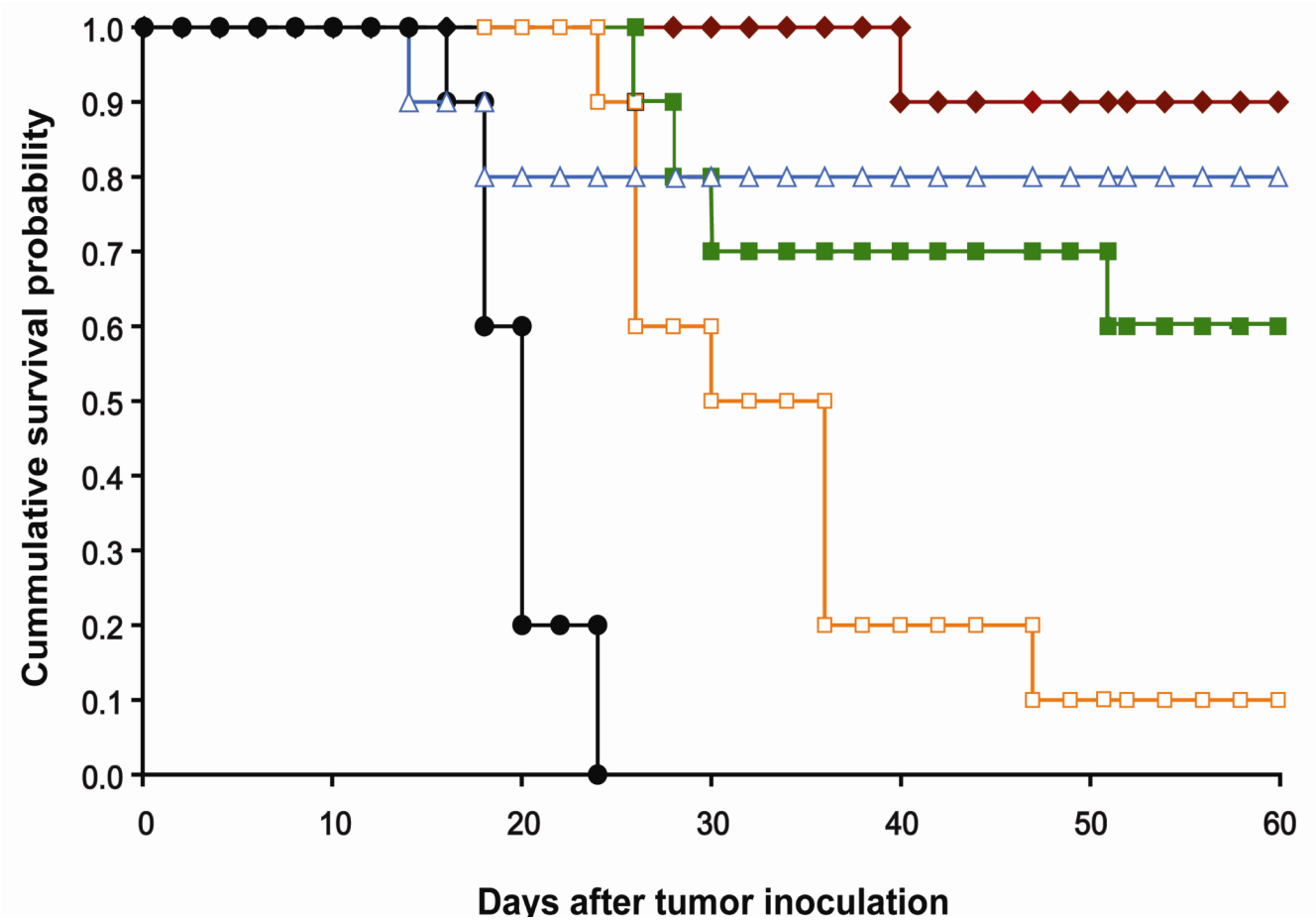


**Figure 5.**

Survival probability versus time for Balb/C mice bearing s.c. C26 colon carcinoma after a single injection of PEGylated polyester-amide Dox conjugate or control. Mice were treated 8 days after tumoring. ♦, **27** (20 mg Dox equiv/kg); ■, **27** (15 mg Dox equiv/kg); □, **27** (10 mg Dox equiv/kg); Δ, Doxil™ (20 mg Dox equiv/kg); ●, PBS.

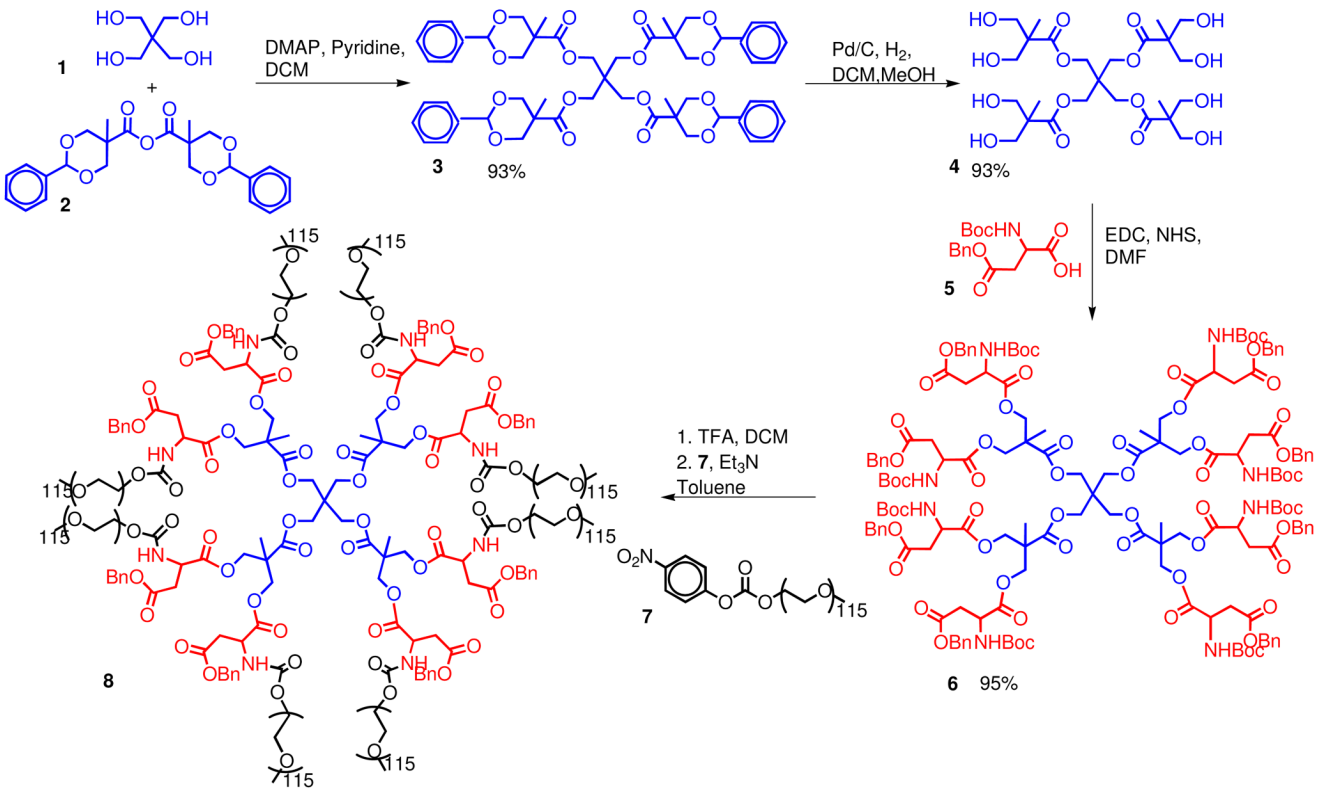


**Scheme 1.**
Synthesis of Symmetrically PEGylated Dendrimer.

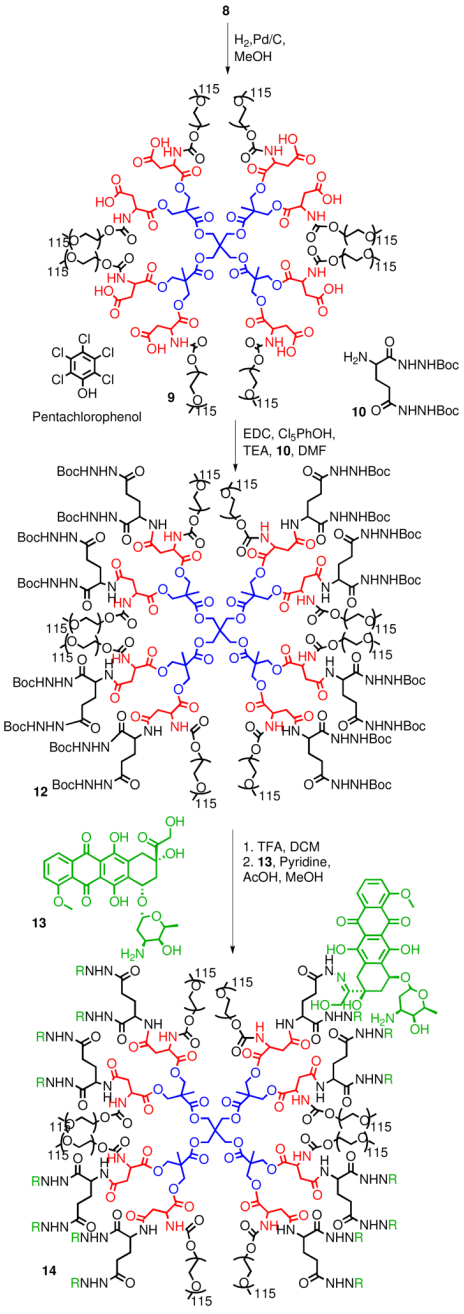


**Scheme 2.**
Linker attachment and Dox loading.

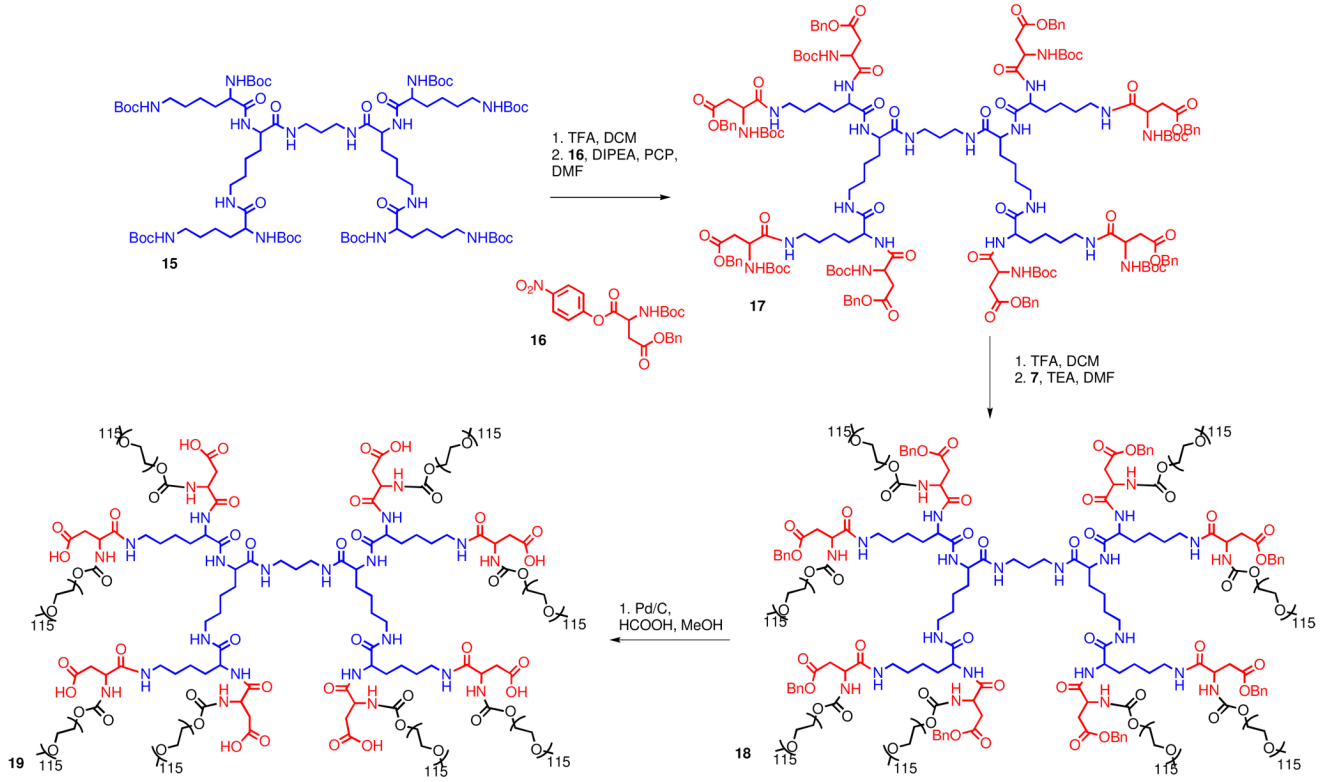


**Scheme 3.**
PEGylated polylysine synthesis.

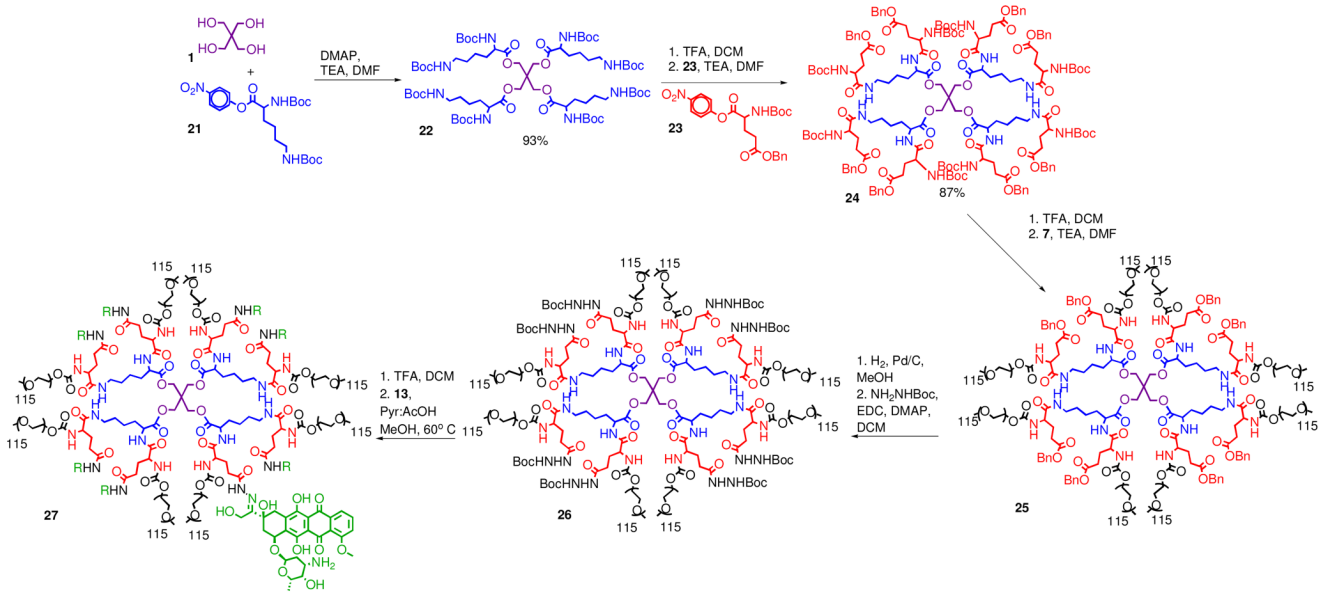


**Scheme 4.**
Synthesis of drug loaded PEGylated ester-amide dendrimer.

**Table 1**

In vivo efficacy of ester amide dendrimer conjugate and controls against Balb/C mice with C26 colon carcinoma.

| Treatment Group | No. mice | Dose (mg/kg) | Mean TGD (%) | Median survival time (days) | TRD | LTS |
|---|---|---|---|---|---|---|
| PBS | 10 | | | 20 | 0 | 0 |
| Doxil™ | 10 | 20 | 245[a] | 60[a] | 2 | 8 |
| **27** | 10 | 20 | 229[a] | 60[a] | 0 | 9 |
| **27** | 10 | 15 | 175[a] | 60[a] | 0 | 6 |
| **27** | 10 | 10 | 74[b] | 33[a] | 0 | 1 |

TGD, tumor growth delay, calculate from time of growth to 400 $mm^3$; TRD, treatment-related death; LTS, long term survivors;

[a] Compared to PBS, $P \leq 0.0001$.

[b] Compared to PBS, $P = 0.004$.

*Bioconjug Chem*. Author manuscript; available in PMC 2011 April 21.